Pyroelectric effect enhancement in laminate composites under short circuit condition

H. H. S. Chang' , R. W. Whatmore, and Z. Huang

Citation: Journal of Applied Physics **106**, 114110 (2009); doi: 10.1063/1.3264623
View online: http://dx.doi.org/10.1063/1.3264623
View Table of Contents: http://aip.scitation.org/toc/jap/106/11
Published by the American Institute of Physics

Pyroelectric effect enhancement in laminate composites under short circuit condition

H. H. S. Chang,[1,a)] R. W. Whatmore,[2] and Z. Huang[1]
[1]*Department of Materials, Cranfield University, Bedfordshire, MK43 0AL, United Kingdom*
[2]*Tyndall National Institute, Lee Maltings, Prospect Row, Cork, Ireland*

(Received 16 January 2009; accepted 24 October 2009; published online 9 December 2009)

The pyroelectric coefficients of laminate composites under short circuit condition have been investigated by analytical modeling and numerical simulations. Indicators for various pyroelectric/non-pyroelectric material pairs that can be utilized to determine their pyroelectric coefficient enhancement credentials have been identified. Six pyroelectric materials were paired with six non-pyroelectric/elastic materials and their pyroelectric coefficient enhancement potential and figure of merit for efficiency were investigated. The best performing partnership out of the 36 pairs was lead zirconate titanate (PZT5H)-chlorinated polyvinyl chloride thermoplastic (CPVC) for thickness ratios (R) below 0.09 and PZT5H-zinc for R larger than 0.09 with both demonstrating total pyroelectric coefficient of approximately -20×10^{-4} C m^{-2} K^{-1} at R=0.09, which corresponds to approximately 300% increase in the coefficient. PZT5H-CPVC also showed maximum of 800% rise in the pyroelectric coefficient while figure of merit for efficiency indicated up to twentyfold increase in its electrical response output per given thermal stimuli when compared to that of PZT5H by itself. © *2009 American Institute of Physics*. [doi:10.1063/1.3264623]

I. INTRODUCTION

The pyroelectric (PY) effect describes a change in the charge density of a material upon thermal stimulus, which can occur in any material with a polar symmetry. Its applications range from thermal radiation detection to fire alarms, intruder detection, and thermal imaging. The pyroelectric coefficient (PY coef.), usually measured at constant stress $p^{T,E}$, consists of the primary PY coef. at the constant strain $p^{S,E}$ and the secondary PY coef. arising from strain,[1]

$$p_m^{T,E} = p_m^{S,E} + d_{mkl}^{E,\Theta} c_{ijkl}^{E,\Theta} \alpha_{ij}^{T,E}. \quad (1)$$

Here, $d_{mkl}^{E,\Theta}$ is the piezoelectric constant, $c_{ijkl}^{E,\Theta}$ is the elastic stiffness, $\alpha_{ij}^{T,E}$ is the thermal expansion coefficient, E is the electric field, and Θ is the temperature. Notice the use of Einstein summation convention which is used throughout this article along with Voigt notation.

A number of researches on the secondary PY coef. can be found in the literature.[2,3] For instance, the effect of a substrate on PY thin films, arising from thermal expansion mismatch, has been investigated extensively by various researchers.[3–7] Generally speaking, for perovskite-based ferroelectric materials the product term $d_{mkl}^{E,\Theta}\ c_{ijkl}^{E,\Theta}\ \alpha_{ij}^{T,E}$ is much smaller than the primary term $p^{S,E}$ and hence the effect of this mismatch is expected to be rather limited.[4,7] The possibility of utilizing secondary PY effect to enhance the total PY coef. was researched by Newnham *et al.*[8] and Nan.[9] Their works led to the development of various composites with superior mechanical flexibility accompanied by good PY performances.[10–14] They concluded that in most cases due to the small hydrostatic piezoelectric effect, arising from cancellation between coefficients of opposite signs, the enhancement available through the secondary contribution is rather limited.

In our previous communication, we reported a substantial PY coef. enhancement in laminar stainless steel/lead zirconate titanate (PZT)/stainless steel structures.[15] With both experimental observation and theoretical prediction demonstrating PY coef. enhancements of more than 100%, we attributed this large enhancement to dissimilar signs of the piezoelectric coefficients of PZT and the exploitation of this particular symmetry through deployment of 2–2 connectivity configuration, where externally exerted strains by the non-pyroelectric (NP) elastic layer, namely, stainless steel, are transferred through in two axes resulting in cumulative piezoelectricity arising from three separate axes owing to Poisson effect.

This dissimilarity in piezoelectric coefficient signs also results in small hydrostatic piezoelectric effect, which in turn lead to the previously held belief that for materials such as PZT the expected gain in PY coef. through its secondary effect would be rather limited.[4,8,9] As our research so far seems to suggest to the contrary, we believe this employment of 2–2 connectivity configuration in pyroelectricity requires further exploration, which could potentially uncover PY coef. enhancements of even greater proportions.

At the outset in Sec. II, we first examine the theoretical and mathematical background behind this subject by applying thermodynamic and plate theory, results of which are presented in later section with the use of Mathematics package MAPLE 9.50.[16] In order to analyze the effects of increased thermal mass due to the introduction of NP elastic layer, we also define a quantity termed efficiency and utilize it to assess the trade-off between increased thermal mass and PY response by defining a figure of merit for efficiency.

Section III consists of a brief introduction to the materials considered for our simulation. This should clarify the

a)Electronic mail: h.chang@cranfield.ac.uk.

reasons behind the choice of our materials, illustrating various relevant properties they possess. The outcomes of the ensuing mathematical simulations and corresponding conclusions are demonstrated in Secs. IV and V.

II. GENERAL THEORETICAL ANALYSIS

A. Pyroelectric coefficient under short circuit condition

To enable the mathematical model to describe our enhancement, a more general case of the above expression (1) needs to be derived from the thermodynamic principles since the final configuration will consist of a PY material attached to a thermally active NP material, which will then exert "thermally motivated external" stress onto the PY material. This implies previous model for PY coef. given by Eq. (1)[1,2,8,17–21] does not supply sufficient enough description of the mechanisms behind our desired effect. So, we derive the expression for the PY coef. (p_i) from its fundamental definition;[1,2] $p_i=\Delta P_{Si}/\Delta\Theta=dP_{Si}/d\Theta$, $i=1\ldots3$, where dP_{Si} is the change in spontaneous polarization vector's component in i-direction, $d\Theta$ is the change in temperature, ΔP_{Si} is the dipole moment per unit volume, i.e., spontaneous polarization, in i-direction, $\Delta\Theta$ is the uniform temperature change, and p_i is the PY coef. in i-direction. Also, $\mathbf{D}=\varepsilon_0\mathbf{E}+\mathbf{P}$ in any dielectric material and $\mathbf{P}=\mathbf{P_S}+\mathbf{P_{Ind}}$ in piezo- or PY materials with $\mathbf{P_{Ind}}=\varepsilon_0\,\boldsymbol{\chi_e}\,\mathbf{E}$,[22] implying $\mathbf{D}=\varepsilon_0\,\boldsymbol{\varepsilon_r}\,\mathbf{E}+\mathbf{P_S}$ and hence $P_{Si}=D_i-\varepsilon_0(\varepsilon_r)_iE_i$. Therefore for short circuit condition ($dE_i=0$),

$$p_i = dP_{Si}/d\Theta = dD_i/d\Theta, \tag{2}$$

where $\mathbf{P}$ is the total polarization, $\mathbf{P_S}$ is the spontaneous polarization, $\mathbf{D}$ is the electric displacement, $\mathbf{E}$ is the electric field (intensity), $\mathbf{P_{Ind}}$ is the induced polarization owing to $\mathbf{E}$, $\boldsymbol{\chi_e}=\boldsymbol{\varepsilon_r}-\mathbf{I}$ is the dielectric susceptibility, $\mathbf{I}$ is the identity matrix/vector, ε_0 is the permittivity of free space, and $\boldsymbol{\varepsilon_r}$ is the relative dielectric constant.

Now, define Gibbs free energy, G, of a piezoelectric crystal as[1,18] $G=U-S_{ij}T_{kl}-D_mE_n-\sigma\Theta$ where $i,j,k,l,m,n=1\ldots3$. Also defining the temperature, stress, and electric field as the independent variables, we have $G=G(T_{ij},E_m,\Theta)$ and assuming constant external electric field (i.e., $dE_n=0$ for all n) for short circuit condition,

$$\begin{aligned} dS_{ij} &= (\partial S_{ij}/\partial T_{kl})_{E,\Theta}dT_{kl} + (\partial S_{ij}/\partial E_n)_{T,\Theta}dE_n \\ &\quad + (\partial S_{ij}/\partial\Theta)_{T,E}d\Theta \\ &= (\partial S_{ij}/\partial T_{kl})_{E,\Theta}dT_{kl} + (\partial S_{ij}/\partial\Theta)_{T,E}d\Theta, \end{aligned}$$

$$\begin{aligned} dD_m &= (\partial D_m/\partial T_{kl})_{E,\Theta}dT_{kl} + (\partial D_m/\partial E_n)_{T,\Theta}dE_n \\ &\quad + (\partial D_m/\partial\Theta)_{T,E}d\Theta \\ &= (\partial D_m/\partial T_{kl})_{E,\Theta}dT_{kl} + (\partial D_m/\partial\Theta)_{T,E}d\Theta, \end{aligned}$$

which implies $dT_{kl}=(\partial S_{ij}/\partial T_{kl})^{-1}_{E,\Theta}[dS_{ij}-(\partial S_{ij}/\partial\Theta)_{T,E}d\Theta]$ and hence

$$\begin{aligned} dD_m &= (\partial D_m/\partial T_{kl})_{E,\Theta}(\partial S_{ij}/\partial T_{kl})^{-1}_{E,\Theta}[dS_{ij} \\ &\quad - (\partial S_{ij}/\partial\Theta)_{T,E}d\Theta] + (\partial D_m/\partial\Theta)_{T,E}d\Theta. \end{aligned} \tag{3}$$

From Eqs. (2) and (3) we get

$$\begin{aligned} p_m &= \frac{dD_m}{d\Theta} = (\partial D_m/\partial\Theta)_{T,E} \\ &\quad - (\partial D_m/\partial T_{kl})_{E,\Theta}(\partial S_{ij}/\partial T_{kl})^{-1}_{E,\Theta}[(\partial S_{ij}/\partial\Theta)_{T,E} \\ &\quad - dS_{ij}/d\Theta] = p_m^{T,E} - (d_{mkl}^{E,\Theta})(s_{ijkl}^{E,\Theta})^{-1}\left[\alpha_{ij}^{T,E} - \frac{dS_{ij}}{d\Theta}\right] \\ &= p_m^{T,E} - (d_{mkl}^{E,\Theta})(c_{ijkl}^{E,\Theta})\left[\alpha_{ij}^{T,E} - \frac{dS_{ij}}{d\Theta}\right], \end{aligned} \tag{4}$$

where p_m is the PY coef., $s_{ijkl}^{E,\Theta}$ is the elastic compliance at constant temperature and electric field, and dS_{ij} is the total strain experienced by the PY material.

It is evident from Eq. (4) that larger the strain the NP component can exert on PY component and greater the piezoelectric coefficient of the PY material, bigger the change in secondary contribution. This leads to the conclusion that stiffer NP material with greater disparity in thermal expansion coefficient (α) with that of PY and more compliant PY material with high piezoelectric coefficients would be desirable.

B. Force balance equation and its solution

Plate theory[23] and force balance equations were used to elicit the strain NP can exert on PY. As the system is symmetrical about the 1–2 plane, two layer plate theory should present a good approximation to our three layer case. From the generalized Hooke's law for orthotropic materials[23] with the assumptions of the Kirchhoff plate conditions,[24] i.e., only S_1, S_2, S_3, and S_6 are non-zero (but $T_3=T_4=T_5=0$), and that the shear stress in 1–2 plane, i.e., $T_6=\tau_{12}$ is negligible, the total strain experienced by PY can be derived.

1. Solving the force balance equation

In general, any solid material has the following elastic relations between the strain (S_j) and stress (T_k): $S_j=\Sigma_{k=1}^{6}s_{jk}T_k$ and $T_k=\Sigma_{j=1}^{6}c_{kj}S_j$. However the Kirchhoff plate conditions and our assumption on the shear stress in 1–2 plane implies we only need to consider S_j for $j=1\ldots3$ and T_k for $k=1\ldots2$. Hence, $S_j=\Sigma_{k=1}^{2}s_{jk}T_k$ and $T_k=\Sigma_{j=1}^{3}c_{kj}S_j$.

Using force balance law at the interface we get the force balance equations parallel to i-axis as

$$\begin{aligned} 0 &= {}^{PY}F_1 + {}^{NP}F_1 = {}^{PY}F_2 + {}^{NP}F_2 = {}^{PY}T_1\,{}^{PY}A_1 + {}^{NP}T_1\,{}^{NP}A_1 \\ &= {}^{PY}T_2\,{}^{PY}A_2 + {}^{NP}T_2\,{}^{NP}A_2 \\ \Rightarrow 0 &= \left[\sum_{j=1}^{3}{}^{PY}c_{ij}\,{}^{PY}S_j\right]{}^{PY}A_i + {}^{NP}T_i\,{}^{NP}A_i \quad \text{for} \quad i=1\ldots2 \end{aligned} \tag{5}$$

where A_i=surface area perpendicular to i-axis and F_i=force acting perpendicular to A_i and along the i-axis.

Now, for ${}^{NP}T_k$ for $k=1\ldots2$, in general the stiffness matrix of a NP material is unknown, therefore we use general plate theory:

$$\begin{pmatrix} {}^{NP}S_1 \\ {}^{NP}S_2 \\ {}^{NP}S_3 \end{pmatrix} = \begin{pmatrix} 1/E_1 & -\nu_{21}/E_2 & -\nu_{31}/E_3 \\ -\nu_{12}/E_1 & 1/E_2 & -\nu_{32}/E_3 \\ -\nu_{13}/E_1 & -\nu_{23}/E_2 & 1/E_3 \end{pmatrix} \begin{pmatrix} {}^{NP}T_1 \\ {}^{NP}T_2 \\ {}^{NP}T_3 = 0 \end{pmatrix}$$

$$\Rightarrow {}^{NP}T_1 = E_1({}^{NP}S_1 + \nu_{21}\,{}^{NP}S_2)/(1-\nu_{21}\nu_{12}) = X_1\,{}^{NP}S_1 + X_2\,{}^{NP}S_2$$

$${}^{NP}T_2 = E_2({}^{NP}S_2 + \nu_{12}\,{}^{NP}S_1)/(1-\nu_{21}\nu_{12}) = Y_1\,{}^{NP}S_1 + Y_2\,{}^{NP}S_2$$

where $X_1 = E_1/(1-\nu_{21}\nu_{12})$, $X_2 = E_1\nu_{21}/(1-\nu_{21}\nu_{12})$, $Y_1 = E_2\nu_{12}/(1-\nu_{21}\nu_{12})$, and $Y_2 = E_2/(1-\nu_{21}\nu_{12})$.

Therefore, Eq. (5) becomes

$$0 = \left[\sum_{j=1}^{3} {}^{PY}c_{1j}\,{}^{PY}S_j\right]{}^{PY}A_1 + [X_1\,{}^{NP}S_1 + X_2\,{}^{NP}S_2]{}^{NP}A_1,$$

$$0 = \left[\sum_{j=1}^{3} {}^{PY}c_{2j}\,{}^{PY}S_j\right]{}^{PY}A_2 + [Y_1\,{}^{NP}S_1 + Y_2\,{}^{NP}S_2]{}^{NP}A_2. \tag{6}$$

Also, the strain in three direction can be expressed as

$$\begin{aligned} {}^{PY}S_3 &= s_{31}T_1 + s_{32}T_2 = s_{31}(c_{11}\,{}^{PY}S_1 + c_{12}\,{}^{PY}S_2 + c_{13}\,{}^{PY}S_3) \\ &\quad + s_{32}(c_{21}\,{}^{PY}S_1 + c_{22}\,{}^{PY}S_2 + c_{23}\,{}^{PY}S_3) = [(s_{31}c_{11} \\ &\quad + s_{32}c_{21})^{PY}S_1 + (s_{31}c_{12} + s_{32}c_{22})^{PY}S_2]/[1-(s_{31}c_{13} \\ &\quad + s_{32}c_{23})] = {}^{PY}\Lambda_1\,{}^{PY}S_1 + {}^{PY}\Lambda_2\,{}^{PY}S_2, \end{aligned}$$

where

$${}^{PY}\Lambda_1 = (s_{31}c_{11} + s_{32}c_{21})/[1-(s_{31}c_{13} + s_{32}c_{23})] \text{ and}$$

$${}^{PY}\Lambda_2 = (s_{31}c_{12} + s_{32}c_{22})/[1-(s_{31}c_{13} + s_{32}c_{23})]. \tag{7}$$

The dimensions for each material at each temperature state to be considered are (henceforth in this section all the expressions are true for $j=1\ldots2$ unless stated otherwise):

Case (a). This is the initial state of the composite (at initial temperature Θ_1): ${}^{PY}l_j^I, {}^{PY}A_j^I, {}^{NP}l_j^I, {}^{NP}A_j^I$.

Case (b). Composite is not bonded; however, the thermal expansion has taken place separately for each PY and NP material (initial state for force balance equation where temperature has been raised to the required higher level, Θ_2):

$${}^{PY'}l_j^{II}, {}^{PY'}A_j^{II}, {}^{NP'}l_j^{II}, {}^{NP'}A_j^{II} \Rightarrow {}^{PY'}l_j^{II} = {}^{PY}l_j^I(1 + {}^{PY}\alpha_j d\Theta)$$

$$\text{and } {}^{NP'}l_j^{II} = {}^{NP}l_j^I(1 + {}^{NP}\alpha_j d\Theta). \tag{8}$$

Case (c). This is the actual final state of bonded composite which is at equilibrium (final state for force balance equation with temperature still at the higher level, Θ_2):

$${}^{PY}l_j^{II}, {}^{PY}A_j^{II}, {}^{NP}l_j^{II}, {}^{NP}A_j^{II} \Rightarrow \text{Min}({}^{PY'}l_j^{II}, {}^{NP'}l_j^{II}) < {}^{PY}l_j^{II} = {}^{NP}l_j^{II} < \text{Max}({}^{PY'}l_j^{II}, {}^{NP'}l_j^{II}). \tag{9}$$

Solving of the force balance equation is required to obtain these lengths at equilibrium (i.e., final lengths for the bonded samples). Once the force balance equation is solved, the resulting expressions will lead us to the final strain terms arising from the interaction between the two constituents.

In order to acquire strain expressions for the force balance equation (Note: ${}^{PY}S_j$ and ${}^{NP}S_j$ in force balance equation are when ${}^{PY}l_j^{II}$ and ${}^{NP}l_j^{II}$ are achieved.) at Θ_2, force balance must occur: initial state for force balance equation [Case (b)] $\equiv {}^{PY'}l_j^{II}, {}^{NP'}l_j^{II}$, final state for force balance equation [Case (c)] $\equiv {}^{PY}l_j^{II}, {}^{NP}l_j^{II} = L_j^{II}$ (NB: since bonded, ${}^{PY}l_j^I = {}^{NP}l_j^I = L_j^I$ as well).

From Eq. (8) the strains in terms of lengths: ${}^{PY'}l_j^{II} = L_j^I(1 + {}^{PY}\alpha_j d\Theta)$ and ${}^{NP'}l_j^{II} = L_j^I(1 + {}^{NP}\alpha_j d\Theta)$

$\Rightarrow$Strains at final state are

$${}^{PY}S_j = [L_j^{II} - L_j^I(1 + {}^{PY}\alpha_j d\Theta)]/[L_j^I(1 + {}^{PY}\alpha_j d\Theta)]$$

and

$${}^{NP}S_j = [L_j^{II} - L_j^I(1 + {}^{NP}\alpha_j d\Theta)]/[L_j^I(1 + {}^{NP}\alpha_j d\Theta)]. \tag{10}$$

Before solving the force balance equation, we require another relationship between ${}^{PY}S_j$ and ${}^{NP}S_j$. Solving Eq. (10) for L_j^{II}:

$$\Rightarrow L_j^{II} = ({}^{PY}S_j + 1)L_j^I(1 + {}^{PY}\alpha_j d\Theta) = ({}^{NP}S_j + 1)L_j^I(1 + {}^{NP}\alpha_j d\Theta)$$

$$\Rightarrow {}^{PY}S_j = \frac{({}^{NP}S_j + 1)(1 + {}^{NP}\alpha_j d\Theta)}{(1 + {}^{PY}\alpha_j d\Theta)} - 1 = \frac{{}^{NP}S_j(1 + {}^{NP}\alpha_j d\Theta) + ({}^{NP}\alpha_j - {}^{PY}\alpha_j)d\Theta}{(1 + {}^{PY}\alpha_j d\Theta)} \text{ and}$$

$${}^{NP}S_j = \frac{({}^{PY}S_j + 1)(1 + {}^{PY}\alpha_j d\Theta)}{(1 + {}^{NP}\alpha_j d\Theta)} - 1 = \frac{{}^{PY}S_j(1 + {}^{PY}\alpha_j d\Theta) + ({}^{PY}\alpha_j - {}^{NP}\alpha_j)d\Theta}{(1 + {}^{NP}\alpha_j d\Theta)}. \tag{11}$$

Now, substituting Eq. (11) into Eqs. (6) and (7):

$$\Rightarrow 0 = [c_{11}\,{}^{PY}S_1 + c_{12}\,{}^{PY}S_2 + c_{13}\,{}^{PY}S_3]{}^{PY}A_1 + [X_1\,{}^{NP}S_1 + X_2\,{}^{NP}S_2]{}^{NP}A_1$$

$$= {}^{PY}A_1[c_{11}\,{}^{PY}S_1 + c_{12}\,{}^{PY}S_2 + c_{13}\{{}^{PY}\Lambda_1\,{}^{PY}S_1 + {}^{PY}\Lambda_2\,{}^{PY}S_2\}]$$

$$+ {}^{NP}A_1\left[X_1\frac{{}^{PY}S_1(1 + {}^{PY}\alpha_1 d\Theta) + ({}^{PY}\alpha_1 - {}^{NP}\alpha_1)d\Theta}{(1 + {}^{NP}\alpha_1 d\Theta)} + X_2\frac{{}^{PY}S_2(1 + {}^{PY}\alpha_2 d\Theta) + ({}^{PY}\alpha_2 - {}^{NP}\alpha_2)d\Theta}{(1 + {}^{NP}\alpha_2 d\Theta)}\right]$$

$$= \Omega_{11}\,{}^{PY}S_1 + \Omega_{12}\,{}^{PY}S_2 + {}^{NP}A_1\{X_1\Gamma_{21} + X_2\Gamma_{22}\}$$

$$\text{and } 0 = [c_{21}\,{}^{PY}S_1 + c_{22}\,{}^{PY}S_2 + c_{23}\,{}^{PY}S_3]{}^{PY}A_2 + [Y_1\,{}^{NP}S_1 + Y_2\,{}^{NP}S_2]{}^{NP}A_2$$

$$= {}^{PY}A_2[c_{21}\,{}^{PY}S_1 + c_{22}\,{}^{PY}S_2 + c_{23}\{{}^{PY}\Lambda_1\,{}^{PY}S_1 + {}^{PY}\Lambda_2\,{}^{PY}S_2\}]$$

$$+{}^{NP}A_2\left[Y_1\frac{{}^{PY}S_1(1+{}^{PY}\alpha_1 d\Theta)+({}^{PY}\alpha_1-{}^{NP}\alpha_1)d\Theta}{(1+{}^{NP}\alpha_1 d\Theta)}+Y_2\frac{{}^{PY}S_2(1+{}^{PY}\alpha_2 d\Theta)+({}^{PY}\alpha_2-{}^{NP}\alpha_2)d\Theta}{(1+{}^{NP}\alpha_2 d\Theta)}\right]$$

$$=\Omega_{21}\,{}^{PY}S_1+\Omega_{22}\,{}^{PY}S_2+{}^{NP}A_2\{Y_1\Gamma_{21}+Y_2\Gamma_{22}\}, \quad (12)$$

where $\Gamma_{11}=(1+{}^{PY}\alpha_1 d\Theta)/(1+{}^{NP}\alpha_1 d\Theta)$, $\Gamma_{12}=(1+{}^{PY}\alpha_2 d\Theta)/(1+{}^{NP}\alpha_2 d\Theta)$, $\Gamma_{21}=({}^{PY}\alpha_1-{}^{NP}\alpha_1)d\Theta/(1+{}^{NP}\alpha_1 d\Theta)$, $\Gamma_{22}=({}^{PY}\alpha_2-{}^{NP}\alpha_2)d\Theta/(1+{}^{NP}\alpha_2 d\Theta)$, $\Omega_{11}=\{{}^{PY}A_1(c_{11}+c_{13}\,{}^{PY}\Lambda_1)+{}^{NP}A_1X_1\Gamma_{11}\}$, $\Omega_{12}=\{{}^{PY}A_1(c_{12}+c_{13}\,{}^{PY}\Lambda_2)+{}^{NP}A_1X_2\Gamma_{12}\}$, $\Omega_{21}=\{{}^{PY}A_2(c_{21}+c_{23}\,{}^{PY}\Lambda_1)+{}^{NP}A_2Y_1\Gamma_{11}\}$, and $\Omega_{22}=\{{}^{PY}A_2(c_{22}+c_{23}\,{}^{PY}\Lambda_2)+{}^{NP}A_2Y_2\Gamma_{12}\}$.

It must be noted that ${}^{PY}A_j$ and ${}^{NP}A_j$ (for all $j=1\ldots3$) can also be expressed in terms of ${}^{PY}S_j$ ($j=1\ldots3$). However, this will destroy the linearity of this force balance equation and introduce unnecessary complications. Therefore, it is assumed that the areas remain constant even after the linear thermal expansions in all three directions. Hence, ${}^{PY}A_1=L_2\,{}^{PY}t$, ${}^{PY}A_2=L_1\,{}^{PY}t$, ${}^{NP}A_1=L_2\,{}^{NP}t$, and ${}^{NP}A_2=L_1\,{}^{NP}t$ when ${}^{PY}l_j^I={}^{NP}l_j^I=L_j$, ${}^{PY}l_3^I={}^{PY}t$, and ${}^{NP}l_2^I={}^{NP}t$.

Solving the force balance Eq. (12), in terms of ${}^{PY}S_1$ and ${}^{PY}S_2$, we obtain following expressions:

$$\begin{aligned}
{}^{PY}S_1&=[{}^{NP}A_1\Omega_{22}\{X_1\Gamma_{21}+X_2\Gamma_{22}\}-{}^{NP}A_2\Omega_{12}\{Y_1\Gamma_{21}+Y_2\Gamma_{22}\}]/[\Omega_{12}\Omega_{21}-\Omega_{22}\Omega_{11}],\\
{}^{PY}S_2&=[{}^{NP}A_2\Omega_{11}\{Y_1\Gamma_{21}+Y_2\Gamma_{22}\}-{}^{NP}A_1\Omega_{21}\{X_1\Gamma_{21}+X_2\Gamma_{22}\}]/[\Omega_{12}\Omega_{21}-\Omega_{22}\Omega_{11}],\\
{}^{PY}S_3&={}^{PY}\Lambda_1\,{}^{PY}S_1+{}^{PY}\Lambda_2\,{}^{PY}S_2=\frac{{}^{NP}A_1\{X_1\Gamma_{21}+X_2\Gamma_{22}\}({}^{PY}\Lambda_1\Omega_{22}-{}^{PY}\Lambda_2\Omega_{21})+{}^{NP}A_2\{Y_1\Gamma_{21}+Y_2\Gamma_{22}\}({}^{PY}\Lambda_2\Omega_{11}-{}^{PY}\Lambda_1\Omega_{12})}{\Omega_{12}\Omega_{21}-\Omega_{22}\Omega_{11}}.
\end{aligned} \quad (13)$$

III. CORRECTION FOR THE STRAIN EXPRESSIONS BEFORE THEY CAN BE APPLIED TO THE PYROELECTRIC COEFFICIENTS

Although we now have the solution for the force balance equation, we must remember that the strain expressions in the force balance equation have different lengths at their initial state [Case (b)] when compared to the strain expression in the PY coef. [Case (a)]. We compensate for this by setting dS_j (strain expression to be substituted into the PY coef.) as the strain with the initial state at ${}^{PY}l_j^I={}^{NP}l_j^I=L_j^I$. However, ${}^{PY}S_j$ in force balance equation is the strain with the initial state at ${}^{PY'}l_j^{II}=L_j^I(1+{}^{PY}\alpha_j d\Theta)\neq{}^{NP'}l_j^{II}=L_j^I(1+{}^{NP}\alpha_j d\Theta)$.

$$\Rightarrow dS_j=(L_j^{II}-L_j^I)/L_j^I \text{ and } {}^{PY}S_j=[L_j^{II}-L_j^I(1+{}^{PY}\alpha_j d\Theta)]/[L_j^I(1+{}^{PY}\alpha_j d\Theta)]$$

$$\Rightarrow \text{after equating for } L_j^{II}, \text{we get}$$

$$\therefore dS_j=[({}^{PY}S_j+1)\{L_j^I(1+{}^{PY}\alpha_j d\Theta)\}-L_j^I]/L_j^I=({}^{PY}S_j+1)\times(1+{}^{PY}\alpha_j d\Theta)-1 \text{ for all } j=1\ldots3. \quad (14)$$

One can now evaluate the PY coef. of any 2–2 connectivity laminate composites by substituting Eqs. (13) into (14) and then putting the resulting expression into Eq. (4).

IV. SIMPLIFIED EXPRESSION FOR THE STRAINS EXPERIENCED BY PY MATERIALS

We can also simplify the strain expression in Eqs. (13) and (14) further by considering the symmetry of our PY materials. Due to limited information available and with the aim of simplifying our mathematical model, the following assumptions are made. For PY material, $s_{13}=s_{23}$, $c_{11}=c_{22}$, $c_{12}=c_{21}$, and $c_{23}=c_{31}$; for both PY and NP material, ${}^{PY}\alpha={}^{PY}\alpha_j$, ${}^{NP}\alpha={}^{NP}\alpha_j$ for all $j=1\ldots3$ and $Y=E_1=E_2$, and $\nu=\nu_{12}=\nu_{21}$.

Applying these assumptions to Eqs. (6), (7), and (12):

$$\begin{aligned}
&\Rightarrow X_1=Y_2=Y/(1-\nu^2), \quad X_2=Y_1=Y\nu/(1-\nu^2),\\
&\Gamma_{11}=\Gamma_{12}=(1+{}^{PY}\alpha d\Theta)/(1+{}^{NP}\alpha d\Theta),\\
&\Gamma_{21}=\Gamma_{22}=({}^{PY}\alpha-{}^{NP}\alpha)d\Theta/(1+{}^{NP}\alpha d\Theta),\\
&{}^{PY}\Lambda_1={}^{PY}\Lambda_2=s_{13}(c_{11}+c_{12})/(1-2s_{13}c_{13})=\Lambda,\\
&\Omega_{11}=\{{}^{PY}A_1(c_{11}+c_{13}\Lambda)+{}^{NP}A_1X_1\Gamma_{11}\},\\
&\Omega_{12}=\{{}^{PY}A_1(c_{12}+c_{13}\Lambda)+{}^{NP}A_1X_2\Gamma_{11}\},\\
&\Omega_{21}=\{{}^{PY}A_2(c_{12}+c_{13}\Lambda)+{}^{NP}A_2X_2\Gamma_{11}\}, \text{ and}\\
&\Omega_{22}=\{{}^{PY}A_2(c_{11}+c_{13}\Lambda)+{}^{NP}A_2X_1\Gamma_{11}\}.
\end{aligned}$$

Now, substituting above stated relations into Eq. (13) along with ${}^{PY}A_1=L_2\,{}^{PY}t$, ${}^{PY}A_2=L_1\,{}^{PY}t$, ${}^{NP}A_1=L_2\,{}^{NP}t$, and ${}^{NP}A_2=L_1\,{}^{NP}t$, we attain the following expression:

$$\Rightarrow {}^{PY}S_1={}^{PY}S_2=({}^{NP}\alpha-{}^{PY}\alpha)d\Theta/\left[\frac{(1-\nu)}{Y}\left(\frac{c_{11}+c_{12}}{1-2s_{13}c_{13}}\right)\times(1+{}^{NP}\alpha d\Theta)R+(1+{}^{PY}\alpha d\Theta)\right] \text{ and}$$

$$
\begin{aligned}
{}^{PY}S_3 &= {}^{PY}\Lambda_1\,{}^{PY}S_1 + {}^{PY}\Lambda_2\,{}^{PY}S_2 = 2\Lambda\,{}^{PY}S_1 \\
&= \left(\frac{2s_{13}(c_{11}+c_{12})}{1-2s_{13}c_{13}}\right)({}^{NP}\alpha \\
&\quad - {}^{PY}\alpha)d\Theta / \left[\frac{(1-\nu)}{Y}\left(\frac{c_{11}+c_{12}}{1-2s_{13}c_{13}}\right)(1+{}^{NP}\alpha d\Theta)R\right. \\
&\quad \left. + (1+{}^{PY}\alpha d\Theta)\right]. \qquad (15)
\end{aligned}
$$

In order to obtain the strain expression to be substituted into the PY coef. expression, substitute Eqs. (15) into (14) to obtain

$$
d\,{}^{PY}S_1 = d\,{}^{PY}S_2 = \frac{Y(1-2s_{13}c_{13})(1+{}^{PY}\alpha d\Theta)({}^{NP}\alpha - {}^{PY}\alpha)d\Theta}{(1-\nu)(c_{11}+c_{12})(1+{}^{NP}\alpha d\Theta)R + Y(1-2s_{13}c_{13})(1+{}^{PY}\alpha d\Theta)} + {}^{PY}\alpha d\Theta \quad \text{and}
$$

$$
d\,{}^{PY}S_3 = \frac{2Ys_{13}(c_{11}+c_{12})(1+{}^{PY}\alpha d\Theta)({}^{NP}\alpha - {}^{PY}\alpha)d\Theta}{(1-\nu)(c_{11}+c_{12})(1+{}^{NP}\alpha d\Theta)R + Y(1-2s_{13}c_{13})(1+{}^{PY}\alpha d\Theta)} + {}^{PY}\alpha d\Theta, \qquad (16)
$$

where Y and ν are the Young's modulus and Poisson's ratio of NP, respectively, s_{ij} is the elastic compliance of PY, c_{ij} is the elastic stiffness of PY, and R is the thickness ratio of PY to NP layers.

Substituting Eqs. (16) into (4) yields the PY coef. of our structures, depicting the performance of our enhancement. It must be noted that although Eqs. (4), (13), and (14) are applicable to any PY material universally, Eqs. (15) and (16) are simplified forms of the solution with certain assumptions of symmetry on the PY material, which all but one, namely, poly-vinylidene fluoride (PVDF), PY materials explored in this article suffice. For PVDF we implemented the full solution to the force balance Eqs. (13) and (14), the consequences of which are elucidated in later sections.

A. Thermal mass and efficiency

Although thermal mass should not be a major concern where an abundant heat energy source exists nearby the PY application, such as in some energy harvesting applications, for others this could play an integral part as the measure of performance.[25] Therefore, we define a measure termed "Efficiency (Eff)" and use it as a measure of how efficiently our PY structures convert heat energy into electricity. Eff = Polarisation change due to PY effect/thermal energy input $= \Delta P_S/(\mathrm{Vol}\times c_{vol}\times\Delta\Theta) = p_3\Delta\Theta/(\mathrm{Vol}\times c_{vol}\times\Delta\Theta) = p_3/(\mathrm{Vol}\times c_{vol})$ measured in C m^{-2} J^{-1}, where ΔP_S is the polarization change, Vol is the volume, c_{vol} is the volumetric heat capacity, and p_3 is the PY coef.

Total thermal energy input of the whole composite = arithmetic sum of each constituent's $\mathrm{Vol}\times c_{vol}\times\Delta\Theta$.[26] Hence, ^{Com}Eff = efficiency of a composite

$$
\begin{aligned}
&= \frac{{}^{Com}(\Delta P_S)}{\text{Total thermal energy input}} \\
&= \frac{({}^{Com}p_3)\Delta\Theta}{\left\{\sum_i[(\mathrm{Vol})_i\times(c_{vol})_i]\right\}\times\Delta\Theta} = \frac{({}^{Com}p_3)}{\left\{\sum_i[(\mathrm{Vol})_i\times(c_{vol})_i]\right\}}, \qquad (17)
\end{aligned}
$$

where ^{Com} denotes "composite" and $(\,)_i$ stands for "of the ith constituent".

With Eff, we can quantify the ratio of electrical energy a material can produce given a unit of thermal energy. Since we only consider 2–2 connectivity structures, we assume all constituents of the structure to have the same length L and width W. As the PY coef. is dependent on the thickness ratio between PY and NP materials (R), it would make sense to have R as the independent variable. In order to derive the efficiency comparison expression, let t_3 be the total thickness of all the constituents added together; $t_3 = {}^{PY}t + {}^{NP}t$ and $R = {}^{PY}t/{}^{NP}t \Rightarrow {}^{PY}t = t_3R/(R+1)$ and ${}^{NP}t = t_3/(R+1)$. Substituting into Eq. (17),

$$
\begin{aligned}
{}^{Com}\mathrm{Eff} &= \frac{({}^{Com}p_3)}{\left[\sum_i((\mathrm{Vol})_i\times(c_{vol})_i)\right]} \\
&= \frac{p(R)}{LW\left[\dfrac{{}^{PY}c_{vol}t_3R}{R+1} + \dfrac{{}^{NP}c_{vol}t_3}{R+1}\right]} \\
&= \frac{p(R)}{\dfrac{t_3LW}{R+1}[{}^{PY}c_{vol}R + {}^{NP}c_{vol}]},
\end{aligned}
$$

where ${}^{PY}t$ is the thickness of PY, ${}^{NP}t$ is the thickness of NP, p(R) is PY coef. as a function of R, and ${}^{PY}c_{vol}$ or ${}^{NP}c_{vol}$ is the volumetric heat capacity of PY or NP.

One can now make a comparison between a PY material by itself and its 2–2 connectivity composite. The simplest way to do this is by ratio. Hence, we define a figure of merit for efficiency by $F_{eff} = {}^{Com}\mathrm{Eff}/{}^{PY}\mathrm{Eff}$, where ^{PY}Eff denotes the efficiency of the pure PY material. Depending on the application, we have derived two different expressions for F_{eff}.

(a) First is the ratio between the same total volume of PY material and 2–2 connectivity composite, namely, F^a_{eff}, which will result in the ratio between a 2–2 connectivity composite and a PY material with the same thickness as the total thickness of the composite (this means

TABLE I. PY materials assessment.

	PZT-5H	PZT-5A	BTO	PVDF
Young's modulus ($\times 10^9$ Nm^{-2})	134.0	147.0	275.1	3.6
dc1 ($C\ m^{-2}$)	−15.879	−11.337	−2.690	0.0355
dc2 ($C\ m^{-2}$)	−15.879	−11.337	−2.690	0.0004
dc3 ($C\ m^{-2}$)	16.002	8.464	3.660	−0.0176
Primary PY coef. ($\times 10^{-4}$ $C\ m^{-2}\ K^{-1}$)	−4.527	−2.432	−1.382	−0.265
Secondary PY coef. ($\times 10^{-4}$ $C\ m^{-2}\ K^{-1}$)	−0.473	−0.568	−0.618	−0.009
PY coef. Before enhancement ($\times 10^{-4}$ $C\ m^{-2}\ K^{-1}$)	−5.000	−3.000	−2.000	−0.274
Largest PY coef. after enhancement at R=0.2 ($\times 10^{-4}$ $C\ m^{-2}\ K^{-1}$)	−18.7	−11.5	−3.40	−0.301

the thickness of the PY material used in the composite is thinner than the stand alone PY material). Assume the total volume for both cases to be t_3LW:

$$F^a_{eff} = \frac{^{Com}Eff}{^{PY}Eff} = \frac{^{Com}p_3/[(^{PY}c_{vol}R + {}^{NP}c_{vol})t_3LW/(R+1)]}{^{PY}p_3/(t_3LW^{PY}c_{vol})} = \frac{^{Com}p_3\,{}^{PY}c_{vol}[R+1]}{^{PY}p_3[{}^{PY}c_{vol}R + {}^{NP}c_{vol}]}, \quad (18)$$

where $^{PY}p_3$ is PY coef. of PY material.

If $F^a_{eff} > 1$, then this denotes an improvement in the thermal-to-electrical conversion efficiency compared with that of pure PY material, while $F^a_{eff} < 1$ implies an inferior conversion performance. Since both the composite and the PY material are of the same volume, this ratio will indicate an improvement as long as $^{PY}c_{vol} > {}^{NP}c_{vol}$ and $^{Com}p_3 > {}^{PY}p_3$.

(b) Another ratio is between a PY material and a composite with the PY material of the same thickness. Since $^{PY}t = t_3R/(R+1)$, we have

$$F^b_{eff} = {}^{Com}Eff/{}^{PY}Eff = \frac{^{Com}p_3/[(^{PY}c_{vol}R + {}^{NP}c_{vol})t_3LW/(R+1)]}{^{PY}p_3/(^{PY}tLW^{PY}c_{vol})} = \frac{^{Com}p_3/[(^{PY}c_{vol}R + {}^{NP}c_{vol})t_3LW/(R+1)]}{[(R+1)/(t_3R)][(^{PY}p_3)/(LW^{PY}c_{vol})]} = \frac{^{Com}p_3\,{}^{PY}c_{vol}R}{^{PY}p_3[{}^{PY}c_{vol}R + {}^{NP}c_{vol}]}. \quad (19)$$

Once more, $F^b_{eff} > 1$ signifies rise in efficiency. However, in this case the enhanced PY coef. and augmented thermal mass due to the additional mass of NP material means there is a tradeoff between the increased efficiency from the enhanced PY coef. and the decrease from the additional thermal mass.

V. VARIOUS PY AND NP MATERIALS CONSIDERED

Six different PY and NP materials were paired and analyzed for their enhancement potentials with their extreme thermal expansion coefficients/material stiffness, and/or piezoelectric coefficients in mind. The PY materials investigated are PZT, such as PZT-5H and PZT-5A, barium titanate (BTO), PVDF, and lithium tantalate (LTO) and lithium niobate (LNO) for their deployment in applications such as PY x-ray generation[27,28] and electron accelerators.[29] The analysis on LTO and LNO will mainly be dealt in our other publication[30] since their application utilizes PY coef. under open circuit condition.

Expression (4) is the general PY coef. for any PY material under strain. With the symmetry of our particular choice of PY materials (again, this excludes PVDF) in mind, Eq. (4) can be simplified further to

$$p_3 = p_3^{T,E} - d_{31}^{E,\Theta}\sum_{j=1}^{3}\left[(c_{1j}^{E,\Theta} + c_{2j}^{E,\Theta})\left\{\alpha_j^{T,E} - \frac{dS_j}{d\Theta}\right\}\right] - d_{33}^{E,\Theta}\sum_{j=1}^{3}\left[c_{3j}^{E,\Theta}\left\{\alpha_j^{T,E} - \frac{dS_j}{d\Theta}\right\}\right]. \quad (20)$$

When Eq. (20) is evaluated for a typical PZT, e.g., PZT-5H,[31,32] the sums of $d_{mkl}^{E,\Theta}\,c_{ijkl}^{E,\Theta}$ terms for each direction, i.e., corresponding to dS_1 or dS_2 and dS_3, termed dc1 or dc2 and dc3, are dc1=dc2=−15.9 and dc3=16.0 $C\ m^{-2}$. This implies that positive strains in 1 and 2 directions accompanied by a negative strain in 3 direction would lead to a larger negative secondary contribution, resulting in the greatest PY coef. enhancement. The best configuration for this requirement is a 2–2 connectivity laminate since, with increasing temperature, it can lead to PY material's strains in 1 and 2-axis being positive while strain in 3-axis becomes negative as a consequence of Poisson effect.

These dc1, dc2, and dc3 values are the main indicators of potential PY coef. enhancement. Similar analysis on our PY materials are presented in Table I.

As depicted in Table II, PVDF has rather anisotropic thermal expansion behavior due to its uniaxial orientation with very large thermal expansion coefficients. Although the minute size of Young's modulus suggests potential for high

TABLE II. Thermal coefficients of various PY materials (units: $-\alpha$; $\times 10^{-6}$ $m\ m^{-1}\ K^{-1}$-c_{vol}; $\times 10^6$ $Jm^{-3}\ K^{-1}$).

	PZT-5H	PZT-5A	BTO[a]	PVDF
α_1^E	3.0[b]	4.0[b]	15.7	13[c,d]
α_2^E	3.0[b]	4.0[b]	15.7	145[c,d]
α_3^E	3.0[b]	4.0[b]	6.2	80[e]
c_{vol}	3.15[f,g]	3.15[f,g]	3.19	2.3[h]

[a]Reference 46.
[b]Reference 38.
[c]Reference 34.
[d]Reference 45.
[e]Reference 48.
[f]Reference 39.
[g]Reference 49.
[h]Reference 50.

TABLE III. Material properties of NP materials (units: -α; $\times 10^{-6}$ m m^{-1} K^{-1}-c_{vol}; $\times 10^{6}$ Jm^{-3} K^{-1}-Y; $\times 10^{9}$ Nm^{-2}-ν; no unit).

	St[a]	PTFE[b]	CPVC[c]	Al[d,c,e]	Zn[c,f]	Invar36[g,h]
α	14.4	79.0	80.0	24.3	30.2	1.0
c_{vol}	3.91	0.72	1.40	2.40	2.77	5.15
Young's modulus (Y)	193	0.5	3.15[c,i]	73.1	108	141
Poisson's ratio (ν)	0.30	0.46	0.27[j]	0.33	0.25	0.26

[a]Reference 35.
[b]Reference 51.
[c]Reference 52.
[d]Reference 40.
[e]Reference 53.
[f]Reference 54.
[g]Reference 55.
[h]Reference 56.
[i]Reference 57.
[j]Reference 58.

enhancement, it in fact also leads to extremely small dc1, dc2, and dc3 values which result in diminutive secondary contribution. The sum terms dc1, dc2, and dc3 also have opposite signs to that of PZTs insinuating that for PVDF, NP materials of smaller thermal expansion coefficients should introduce enhancement. It must also be noted that the material properties of PVDF varies greatly among different PVDF samples fabricated using dissimilar preparation techniques.[33,34] As different sources attribute different proportions of the total PY coef. to the secondary effect, Kepler and Anderson[34] approximately half and Nix *et al.*[33] at only 10%–60%; the absolute magnitude of our secondary contribution must be considered with these conflicting views in mind. This is the reason why the comparison of the enhancement in PVDF is made in terms of percentile enhancement of the secondary contribution alone rather than the absolute magnitude, the conclusions of which is presented in later section.

The NP materials investigated include stainless steel (St),[35] poly-tetrafluoroethylene (PTFE or Teflon), chlorinated polyvinyl chloride thermoplastic (CPVC), aluminum (Al), zinc (Zn), and Invar 36 (Invar36) whose most important property is its low thermal expansion coefficient, making it the perfect NP material for introducing opposite sign strains in PVDF. The properties of these materials are presented in Table III.

VI. RESULTS AND DISCUSSION

Generally speaking, LTO and LNO displayed relatively small enhancement with similar trends to that of BTO. In addition, PZT-5A also exhibited similar enhancement behavior to that of PZT-5H. In almost all the simulations, Zn outperformed Al when it comes to enhancement and figure of merit for efficiency. Since their difference is quite consistent throughout our investigative thickness range, the pairs with Al are only presented where appropriate.

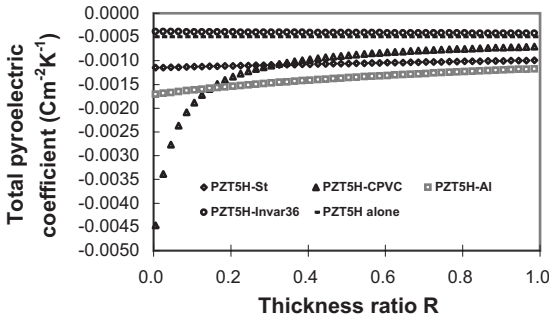

FIG. 1. Total PY coef. vs thickness ratio PY to NP for PZT-5H pairs.

A. PZT-5H

Figure 1 portrays the extreme PY coef. enhancement with CPVC at low R values ($R<0.15$), while at higher R values aluminum outperforms CPVC largely due to much smaller Young's modulus of CPVC. However, it is quite clear that with aluminum or CPVC, one should expect to see much higher PY coef. enhancement than the one with St owing to their superior thermal expansion coefficients as illustrated in Table III. PZT5H-Al pair has the PY coef. of $-0.5\times10^{-3}-[(66\times10^{5})/\{55\times10^{8}+(45\times10^{8})xR\}]$ C m^{-2} K^{-1} and PZT5H-CPVC's is $-0.5\times10^{-3}-[(94\times10^{4})/\{22\times10^{7}+(45\times10^{8})xR\}]$ C m^{-2} K^{-1}. At $R=0.15$, the PY coef. is approximately -16×10^{-4} C m^{-2} K^{-1} for both pairs while at $R=0.005$ PZT5H-CPVC pair exhibits the maximum PY coef. of -45×10^{-4} C m^{-2} K^{-1}. This value at $R=0.005$ is for the ideal case where there exists no loss at the interfacial layer, which in reality is probably difficult to achieve. However, it demonstrates the magnitude of enhancement potential in PZT-5H since its PY coef. without enhancement is -5.0×10^{-4} C m^{-2} K^{-1} as illustrated in Table IV.

The efficiency (F^{a}_{eff}) increase illustrated in Fig. 2 is also very large. At extremely low R of 0.005, F^{a}_{eff} peaks at 20 for PZT5H-CPVC pair, indicating a twentyfold increase in efficiency. PZT5H-Al overtakes PZT5H-CPVC pair at $R=0.35$ with F^{a}_{eff} of 3.5 and continues to outperform the latter at higher R values. This could be important in applications such

TABLE IV. PY coefs. and dielectric constants of various PY materials (units: -$P_3^{T,E}$; $\times10^{-4}$ C m^{-2} K^{-1}-$P_1^{T,E}=0=P_2^{T,E}$-ε; no unit).

	PZT-5H[a,b]	PZT-5A[a,b]	BTO[c,d,e]	PVDF[f,g]
$P_3^{T,E}$	−5.0	−3.0	−2.0	−0.274
ε_{11}^{T}	2438	1796	2920	7.35
ε_{22}^{T}	2438	1796	2920	9.27
ε_{33}^{T}	2874	1803	168	7.75

[a]Reference 38.
[b]Reference 39.
[c]Reference 40.
[d]Reference 41.
[e]Reference 44.
[f]Reference 43.
[g]Reference 45.

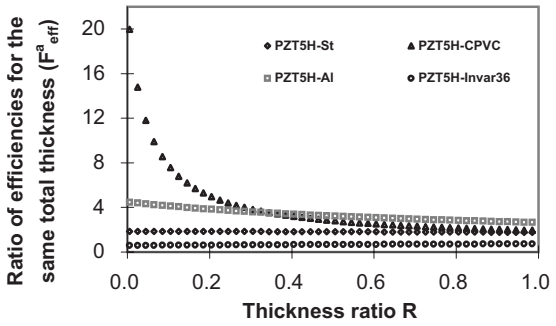

FIG. 2. Efficiency ratios for the same volume of composites and PY material alone vs thickness ratio PY to NP for PZT-5H pairs.

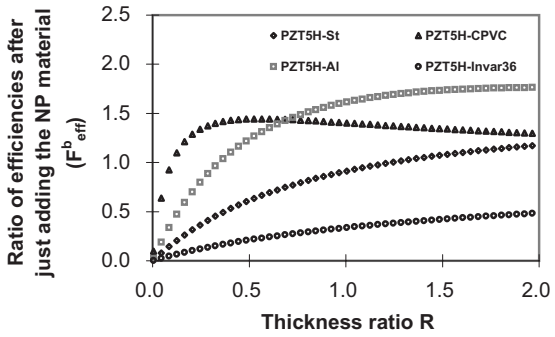

FIG. 3. Efficiency ratios when NP material is added to PY material vs thickness ratio PY to NP for PZT-5H pairs.

as PY sensors.[2,36] In particular, the large efficiency increases at extremely low R values suggest a thin PZT-5H on CPVC substrate may find potential application in PY sensors. Even for the figure of merit for efficiency between PY material alone and NP material added on top (F^b_{eff}), as illustrated in Fig. 3, PZT-5H attains values above 1.0, i.e., an improvement, for PTFE, CPVC, Al, and Zn. This means PZT-5H seems very promising in applications where large amount of steady heat energy is readily available, for example in PY electricity production[37] which utilizes industrial residual heat.

B. BTO

Figure 4 describes largely subdued enhancement for BTO due to relatively small dc values when compared to PZT-5H. However, BTO-CPVC displays rather high enhancement for small thickness ratios of $R<0.1$ with a peak of -8.5×10^{-4} C m^{-2} K^{-1} at $R=0.005$, which is a gain of 325%. It then settles to around $-3.0\times10^{-4}\sim-2.5\times10^{-4}$ C m^{-2} K^{-1} for $R>0.1$. As far as F^a_{eff} is concerned, PTFE (Teflon) displays the most promising figure of merit for efficiency at low R values with Al performing the best of the rest, excluding CPVC, which performed only slightly worse than PTFE with similar trends of high values at low R. Where F^b_{eff} of BTO pairs is considered, BTO-PTFE pair has F^b_{eff} approaching 1.11, i.e., 11% increase. This seems to indicate that a thin coating of PTFE on BTO can lead to higher efficiency.

C. PVDF

As PVDF is a polymer with rather high thermal expansion coefficient with dc values of opposite signs from the rest of PY materials investigated so far, it is expected to behave rather differently from others. The total magnitude of the enhancement is rather small for PVDF. However, Fig. 5 demonstrates how much of an improvement the introduction of NP elastic layer has had on the secondary PY coef. of PVDF with PVDF-Invar36 pair presenting the greatest gain of 260%–300% and PVDF-St pair also performing well at about 200% increase level. This method of comparison may be better suited since the secondary contribution of PVDF's PY coef. varies quite significantly from a sample of PVDF to another, owing largely to their preparation process. The material data used for our simulation were for a PVDF with secondary contribution of only 3.25% of the overall PY coef. Hence if we can achieve similarly high percentile secondary PY coef. enhancement for PVDF samples with larger proportion of secondary contribution such as those presented by Kepler and Anderson,[34] one could expect to see a significantly large enhancement in overall PY coef. Noticeably, Fig. 5 portrays the maximum of 300% enhancement in the secondary PY coef. for PVDF-Invar36 pair, which potentially could lead to extremely large enhancement in other PVDF samples with higher proportion of secondary contribution. Where F^a_{eff} is concerned, Fig. 6 shows PVDF-PTFE demonstrating relatively good values of nearly 3 at very low R, suggesting an improvement in efficiency owing almost entirely to very small heat capacity of PTFE (Table III). However, other pairs struggle to approach one due to already rather low heat capacity of PVDF and very small magnitude of enhancement in comparison. All F^b_{eff} values for PVDF pairs struggle to achieve values higher than one as well. Therefore, among all the PY materials analyzed PVDF is the worst performer when it comes to efficiencies, which is not too surprising since the overall magnitude of enhancement was small.

D. Best performing pairs

In general, for PZT-5H Zn's secondary PY coef. (demonstrated in Fig. 7) is around 25%–45% higher than that of Al depicted in Fig. 1, with the difference getting greater steadily with increasing R. For BTO, Zn's secondary PY coef. is around 35%–45% higher than that of Al, with the difference getting steadily less with increasing R as evident from Figs. 4 and 7. It is evident from Fig. 7 that PZT-5H is

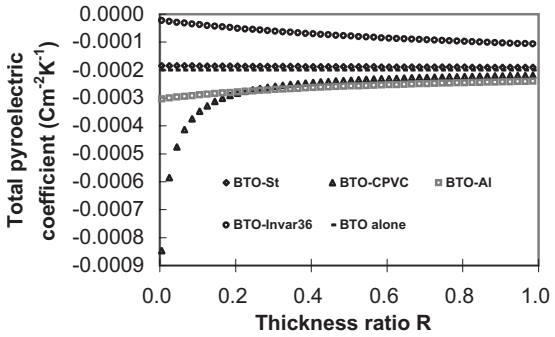

FIG. 4. Total PY coef. vs thickness ratio PY to NP for BTO pairs.

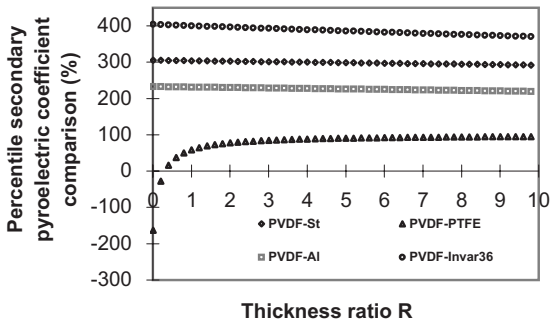

FIG. 5. Percentile secondary contribution from NP material vs thickness ratio PY to NP for PVDF pairs.

by far the best performing material, with CPVC and Zn providing maximum enhancements at $R<0.09$ and $R>0.09$, respectively, while at $R=0.09$ the value for both pairs agree at approximately -20×10^{-4} C m^{-2} K^{-1}. It would be interesting to experimentally verify the extreme PY coef. enhancement of CPVC at very low R values.

Although the enhancement for BTO and PVDF were relatively very small, BTO's enhancement was still up to 325% at very low R range with CPVC and around 65% for high range with Zn. In addition, PVDF showed the best enhancement with Invar36, as expected.

VII. SUMMARY

To summarize, we have analytically modeled 2–2 connectivity composites of PY and NP materials and evaluated the potential PY coefs. of 36 such composites. Paying due consideration to the potential application of such material pairs, indentification has been made on the best possible partnership among these PY and NP materials. In doing so, we have also discovered and confirmed that the sum terms, dc1, dc2, and dc3 are the most viable indicators for determining the feasibility and potential for PY coef. enhancement. The choice of NP material is also found to be dependent on these sum terms, as demonstrated by PVDF-Invar36 pair. Lastly, we have also investigated the additional thermal mass issue of these composites using figure of merit for efficiency with two different cases considered and examined for all 36 pairs.

The best performing partnership out of our 36 PY-NP pairs was PZT5H-CPVC for $R<0.09$ and PZT5H-Zn for $R>0.09$ with both demonstrating approximately 300% increase in total PY coef. at $R=0.09$. PZT5H-CPVC also showed maximum of 800% gain in PY coef. while its F^a_{eff} peaked to 20 and F^b_{eff} to 1.5. For PZT5H-Zn, F^a_{eff} reached maximum of 4.6 and F^b_{eff} of 2.1. All these improvements in efficiencies of PZT-5H insinuates a potential for increased use of PZTs in areas such as PY sensors[36] and PY electricity generation.[37]

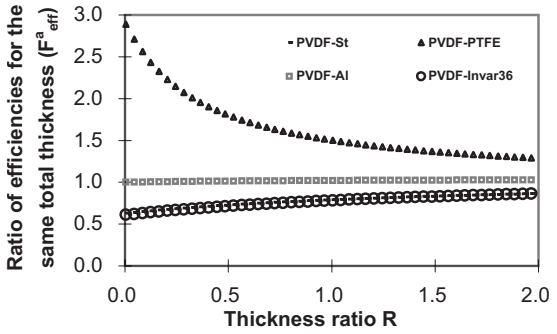

FIG. 6. Efficiency ratios for the same volume of composites and PY material alone vs thickness ratio PY to NP for PVDF pairs.

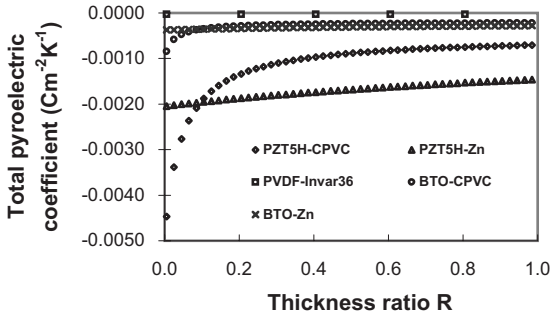

FIG. 7. Total PY coef. vs thickness ratio PY to NP of best performing pairs.

APPENDIX: MATERIAL PARAMETERS OF THE PYROELECTRIC MATERIALS

All the data quoted in this section are evaluated at the room temperature unless stated otherwise.

1. Piezoelectric coefficients

Units: $\times10^{-12}$ CN^{-1}

(a) PZT (Tetragonal, 4 mm)

- PZT-5H[38,39]

$$\underline{d}^E=\begin{pmatrix}0 & 0 & 0 & 0 & 724 & 0\\ 0 & 0 & 0 & 724 & 0 & 0\\ -320 & -320 & 650 & 0 & 0 & 0\end{pmatrix}$$

- PZT-5A[38,39]

$$\underline{d}^E=\begin{pmatrix}0 & 0 & 0 & 0 & 506 & 0\\ 0 & 0 & 0 & 506 & 0 & 0\\ -190 & -190 & 390 & 0 & 0 & 0\end{pmatrix}$$

(b) BTO (Tetragonal, 4 mm)[40,41]

$$\underline{d}^E=\begin{pmatrix}0 & 0 & 0 & 0 & 392 & 0\\ 0 & 0 & 0 & 392 & 0 & 0\\ -34.5 & -34.5 & 85.6 & 0 & 0 & 0\end{pmatrix}$$

(c) PVDF (Orthorhombic, 2 mm)[34,42]

$$\underline{d}^E=\begin{pmatrix}0 & 0 & 0 & 0 & -15.7 & 0\\ 0 & 0 & 0 & d_{24} & 0 & 0\\ 21.4 & 2.3 & -31.5 & 0 & 0 & 0\end{pmatrix}$$

2. Elastic constants

Units: -c^E; $\times10^9$ Nm^{-2} -c^D; $\times10^9$ Nm^{-2}

(a) PZT (Tetragonal, 4 mm)

- PZT-5H[39]

$$\underline{c}^E = \begin{pmatrix} 134 & 89.7 & 85.7 & 0 & 0 & 0 \\ 89.7 & 134 & 85.7 & 0 & 0 & 0 \\ 85.7 & 85.7 & 109 & 0 & 0 & 0 \\ 0 & 0 & 0 & 18.5 & 0 & 0 \\ 0 & 0 & 0 & 0 & 18.5 & 0 \\ 0 & 0 & 0 & 0 & 0 & 22 \end{pmatrix}$$

- PZT-5A[39]

$$\underline{c}^E = \begin{pmatrix} 147 & 105 & 93.7 & 0 & 0 & 0 \\ 105 & 147 & 93.7 & 0 & 0 & 0 \\ 93.7 & 93.7 & 113 & 0 & 0 & 0 \\ 0 & 0 & 0 & 23 & 0 & 0 \\ 0 & 0 & 0 & 0 & 23 & 0 \\ 0 & 0 & 0 & 0 & 0 & 21.2 \end{pmatrix}$$

(b) BTO (Tetragonal, 4 mm)[40,41]

$$\underline{c}^E = \begin{pmatrix} 275.1 & 179 & 151.6 & 0 & 0 & 0 \\ 179 & 275.1 & 151.6 & 0 & 0 & 0 \\ 151.6 & 151.6 & 164.9 & 0 & 0 & 0 \\ 0 & 0 & 0 & 54.34 & 0 & 0 \\ 0 & 0 & 0 & 0 & 54.34 & 0 \\ 0 & 0 & 0 & 0 & 0 & 113.1 \end{pmatrix}$$

(c) PVDF (Orthorhombic, 2 mm)[43,47]

$$\underline{c}^D = \begin{pmatrix} 3.61 & 1.61 & 1.42 & 0 & 0 & 0 \\ 1.61 & 3.13 & 1.31 & 0 & 0 & 0 \\ 1.42 & 1.31 & 1.63 & 0 & 0 & 0 \\ 0 & 0 & 0 & 0.55 & 0 & 0 \\ 0 & 0 & 0 & 0 & 0.59 & 0 \\ 0 & 0 & 0 & 0 & 0 & 0.69 \end{pmatrix}$$

[1] J. F. Nye, *Physical Properties of Crystals* (Oxford University Press, Oxford, 1979).
[2] R. W. Whatmore, Rep. Prog. Phys. **49**, 1335 (1986).
[3] A. Barzegar, D. Damjanovic, N. Ledermann, and P. Muralt, J. Appl. Phys. **93**, 4756 (2003).
[4] J. D. Zook and S. T. Liu, J. Appl. Phys. **49**, 4604 (1978).
[5] A. Sharma, Z.-G. Ban, S. P. Alpay, and J. V. Mantese, J. Appl. Phys. **95**, 3618 (2004).
[6] Z.-G. Ban, S. P. Alpay, A. Sharma, and J. V. Mantese, Appl. Phys. Lett. **84**, 4959 (2004).
[7] P. Muralt, Rep. Prog. Phys. **64**, 1339 (2001).
[8] R. E. Newnham, D. P. Skinner, and E. Cross, Mater. Res. Bull. **13**, 525 (1978).
[9] C.-W. Nan, J. Mater. Sci. Lett. **13**, 1392 (1994).
[10] H. Taunaumang, I. L. Guy, and H. L. W. Chan, J. Appl. Phys. **76**, 484 (1994).
[11] K. S. Lam, Y. W. Wong, L. S. Tai, Y. M. Poon, and F. G. Shin, J. Appl. Phys. **96**, 3896 (2004).
[12] F. Yang, D. Zhang, B. Yu, K. Zheng, and Z. Li, J. Appl. Phys. **94**, 2553 (2003).
[13] K.-H. Chew, F. G. Shin, B. Ploss, H. L. W. Chan, and C. L. Choy, J. Appl. Phys. **94**, 1134 (2003).
[14] Y. Yang, L. W. Chan, and C. L. Choy, J. Mater. Sci. **41**, 251 (2006).
[15] H. H. S. Chang and Z. Huang, Appl. Phys. Lett. **92**, 152903 (2008).
[16] Trademark of Waterloo Maple Inc., in 2004.
[17] N. P. Hartley, P. T. Squire, and E. H. Putley, J. Phys. E **5**, 787 (1972).
[18] M. E. Lines and A. M. Glass, *Applications of Ferroelectrics and Related Materials* (Oxford University Press, Oxford, 1977).
[19] S. B. Lang, Phys. Today, **58** 31 (2005).
[20] R. E. Newnham, D. P. Skinner, K. A. Klicker, A. S. Bhalla, B. Hardiman, and T. R. Gururaja, Ferroelectrics **27**, 49 (1980).
[21] Y. Xu, *Ferroelectric Materials and Their Applications* (North-Holland, Amsterdam, 1991).
[22] B. Wang and C. H. Woo, J. Appl. Phys. **100**, 044114 (2006).
[23] T. Lauwagie, H. Sol, G. Roebben, W. Heylen, Y. Shi, and O. Van der Biest, NDT & E Int. **36**, 487 (2003).
[24] A. E. H. Love, *Mathematical Theory of Elasticity*, 4th ed. (Cambridge University Press, Cambridge, 1927).
[25] W. -M. Lin, Jpn. J. Appl. Phys., Part 1 **41**, 7239 (2002).
[26] K. S. Olofsson, Appl. Compos. Mater. **4**, 1 (1997).
[27] J. D. Brownridge and S. Raboy, J. Appl. Phys. **86**, 640 (1999).
[28] J. D. Brownridge, Nature (London) **358**, 287 (1992).
[29] J. D. Brownridge and S. M. Shafroth, Appl. Phys. Lett. **85**, 1298 (2004).
[30] H. H. S. Chang and Z. Huang, J. Appl. Phys. **106**, 014101 (2009).
[31] For the detailed mechanical properties of both PZTs data from Ferroperm piezoceramics for the corresponding Ferroperm PZTs, namely, Pz27 for PZT-5A and Pz29 for PZT-5H were used, "http://app04.swwwing.net/files/files/Ferroperm%20MatData.xls" in 2006.
[32] For the thermal and piezoelectric properties of PZT-5H (PSI-5H4E) and PZT-5A (PSI-5A4E) values provided by Piezo systems Inc.were used, "http://www.piezo.com/prodmaterialprop.html" in 2006.
[33] E. L. Nix, J. Nanayakkara, G. R. Davies, and I. M. Ward, J. Polym. Sci., Part B: Polym. Phys. **26**, 127 (1988).
[34] R. G. Kepler and R. A. Anderson, J. Appl. Phys. **49**, 4490 (1978).
[35] GoodFellow data provided by Goodfellow was used For the material properties of stainless steel (Stainless steel-15–7PH, "http://www.goodfellow.com/csp/active/gfHome.csp" in 2006.
[36] R. W. Whatmore, P. C. Osbond, and N. M. Shorrocks, Ferroelectrics **76**, 351 (1987).
[37] R. B. Olsen, D. A. Bruno, and J. M. Briscoe, J. Appl. Phys. **58**, 4709 (1985).
[38] For the thermal and piezoelectric properties of PZT-5H (PSI-5H4E) and PZT-5A (PSI-5A4E) values provided by Piezo systems Inc.were used, "http://www.piezo.com/prodmaterialprop.html" in 2006.
[39] For the detailed mechanical properties of both PZTs data from Ferroperm piezoceramics for the corresponding Ferroperm PZTs, namely, Pz27 for PZT-5A and Pz29 for PZT-5H were used, "http://app04.swwwing.net/files/files/Ferroperm%20MatData.xls" in 2006.
[40] eFunda, "http://www.efunda.com/materials/" in 2008.
[41] Edited by K. -H. Hellwege, *Landolt-Bornstein: Numerical Data and Functional Relationships in Science and Technology, Group III: Crystal and Solid State Physics* (Springer-Verlag, Berlin-Heidelberg, 1981).
[42] S. B. Lang and S. Muensit, in Mater. Res. Soc. Symp. Proc. **889**, 01.1 (2006).
[43] Y. Roh, V. V. Varadan, and V. K. Varadan, IEEE Trans. Ultrason. Ferroelectr. Freq. Control **49**, 836 (2002).
[44] A. G. Chynoweth, J. Appl. Phys. **27**, 78 (1956).
[45] Edited by K. -H. Hellwege, *Landolt-Bornstein: Numerical Data and Functional Relationships in Science and Technology, Group III: Crystal and Solid State Physics* (Springer-Verlag, Berlin-Heidelberg, 1982).
[46] H. Surfacenet Gmb, "www.surfacenet.de" in 2003.
[47] H. Y. Guney, J. Polym. Sci. Pol. Phys. **43**, 2862 (2005).
[48] G. D. Sao and H. V. Tiwary, J. Appl. Phys. **53**, 3040 (1982).
[49] D. Berlincourt, H. H. A. Krueger, and C. Near, Report No. TP-226: "Properties of piezoelectricity ceramics," 2003.
[50] H. S. Nalwa, *Ferroelectric Polymers: Chemistry, Physics, and Applications* (Marcel Dekker, Inc., New York, 1995).
[51] Gentech Engineering Plastics, "www.gentechpu.com" in 2008.
[52] Inc. Wikipedia Foundation, "www.wikipedia.com" in 2008.
[53] Ing. Buro R. Tschaggelar, "http://www.ibrtses.com" in 2005.
[54] Goodfellow, "www.goodfellow.com" in 2007.
[55] R. A. Paquin, *Handbook of Optomechanical Engineering* (CRC, Boca Raton, 1997).
[56] R. A. Paquin, *Handbook of Optics*, 2nd ed. (McGraw-Hill, New York, 1995).
[57] N. Merah, M. Irfan-Ul-Haq, and Z. Khan, J. Mater. Process. Technol. **142**, 247 (2003).
[58] B. Scott and K. Michelle, Chem. Eng. Prog. **90**, 36 (1994).